

Electronic Supplementary Information to:

Water desorption from microcline (001): Insights into the first water layer

Tobias Dickbreder,^{a,b} Florian Schneider,^a Lea Klausfering,^a Kim Noelle Dreier,^a Franziska Sabath,^{a,c} Adam S. Foster,^{d,e} Ralf Bechstein,^a Angelika Kühnle^a*

^aPhysical Chemistry I, Faculty of Chemistry, Bielefeld University, Universitätsstraße 25, 33615 Bielefeld, Germany

^bUniversity of Vienna, Department of Chemistry, Institute of Physical Chemistry, Währinger Straße 42, 1090 Vienna, Austria

^cpresent address: Max Planck Institute for Polymer Research, 55128 Mainz, Germany

^dDepartment of Applied Physics, Aalto University, Finland

^eNano Life Science Institute (WPI-NanoLSI), Kanazawa University; Kanazawa 920-1192, Japan

ADDITIONAL AFM DATA

Figure S1 shows all three channels recorded for the AFM image shown in the main part in Figure 1 (a). Figure S2 illustrates the determination of step edge heights. We analyse three exemplary step edges from which one is a single-layer step edge and two are multilayer step edges.

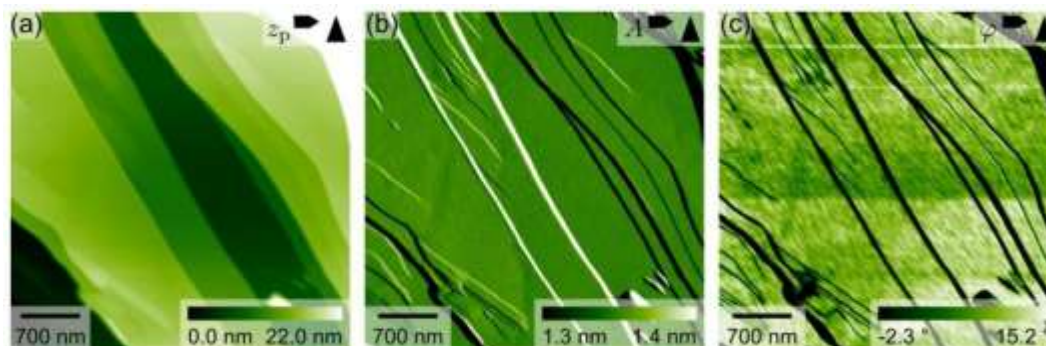


Figure S1: Large-scale AFM image taken at the microcline (001)-water interface in amplitude modulation mode. Shown are the z -piezo displacement (a), oscillation amplitude (b) and phase change (c).

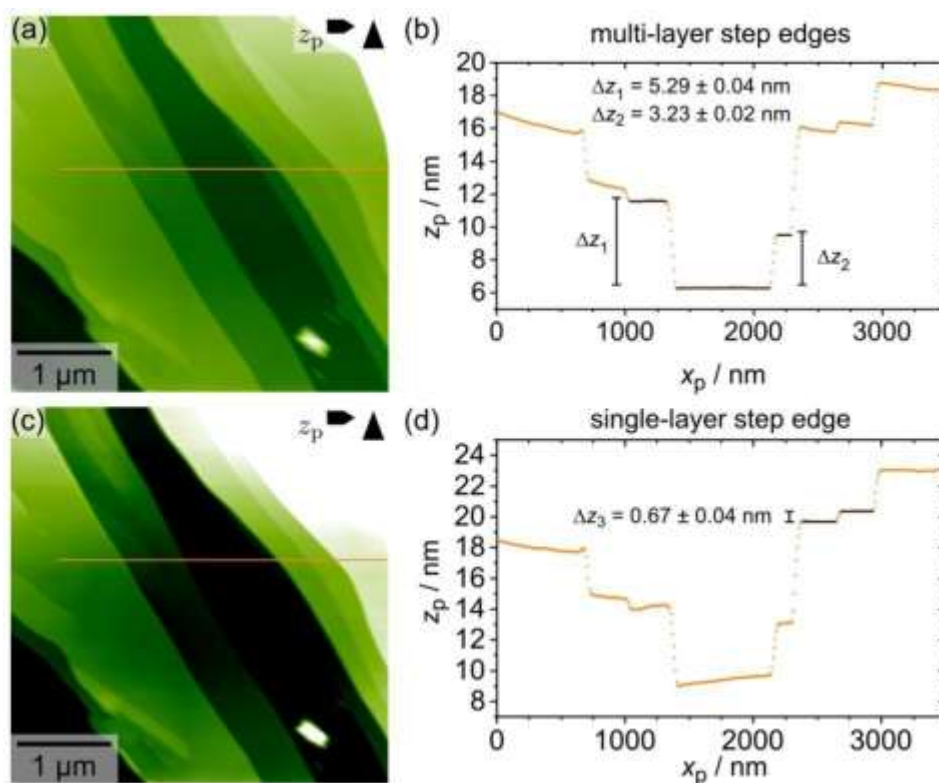


Figure S2: Determination of step edge heights on microcline (001). Step edge heights were determined from profiles extracted along the slow scan direction by averaging the height values measured on the adjacent terraces and

subtracting the mean values. Errors were derived from the standard deviations of the mean terrace heights. Since the images exhibit some non-linear z distortion, a plane level was used to locally level the terraces of interest. (a and b) Levelled image and profile used to extract the heights of multi-layer step edges. The heights of steps 1 and 2 correspond to 8.15 ± 0.06 and 4.97 ± 0.03 layers, respectively. (c and d) Levelled AFM image and profile used to extract the heights of single-layer step edges. The step edge height agrees perfectly with the expected step edge height of 0.649 nm. In the AFM images, profile positions are highlighted in orange.

In Figure 1 (b), we show a cutout of an atomically resolved AFM image taken at the microcline (001) water interface. The full image and all recorded channels of this image are depicted in Figure S3.

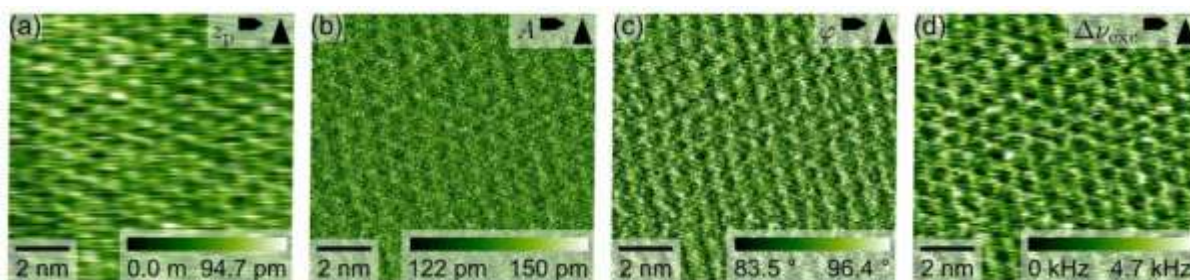


Figure S3: (a) z -Piezo displacement, (b) oscillation amplitude, (c) phase and (d) excitation frequency shift of an atomically resolved frequency modulation AFM image taken at the microcline (001)-water interface. This is the complete AFM image corresponding to the square cutout shown in Fig. 1 (b). The image is drift-corrected and calibrated using unDrift. The z -piezo displacement (a) is corrected by means of mean plane subtraction and row alignment.

WATER DEGASSING AND SAMPLE CLEAVAGE

After bringing the samples into UHV, the sample holder and samples were heated for 3.5 h at up to 750 K to remove contaminations adsorbed on the sample holder and sample. During this step, we observed degassing of mainly water (m/z 18) as shown in the mass spectrum given in Figure S4. After degassing, the samples were cooled down to room temperature, and, then, cleaved by around 35 passes with a tungsten carbide blade. During the cleavage procedure, we monitored the background species with m/z 18 (water) and m/z 28 (probably CO) with the mass spectrometer in the chamber (see Figure S5). The corresponding multiple ion detection (MID) traces show increases in the water background pressure for the cleaving attempts. Unsuccessful cleaving attempts cause a small pressure increase, while the final successful cleavage (blue arrow) causes a

huge pressure increase of two orders of magnitude. These observations suggest that our sample contains significant amounts of water inside its structure, which is consistent with observations reported previously by G. Franceschi *et al.* (Ref. 17 in the main text).

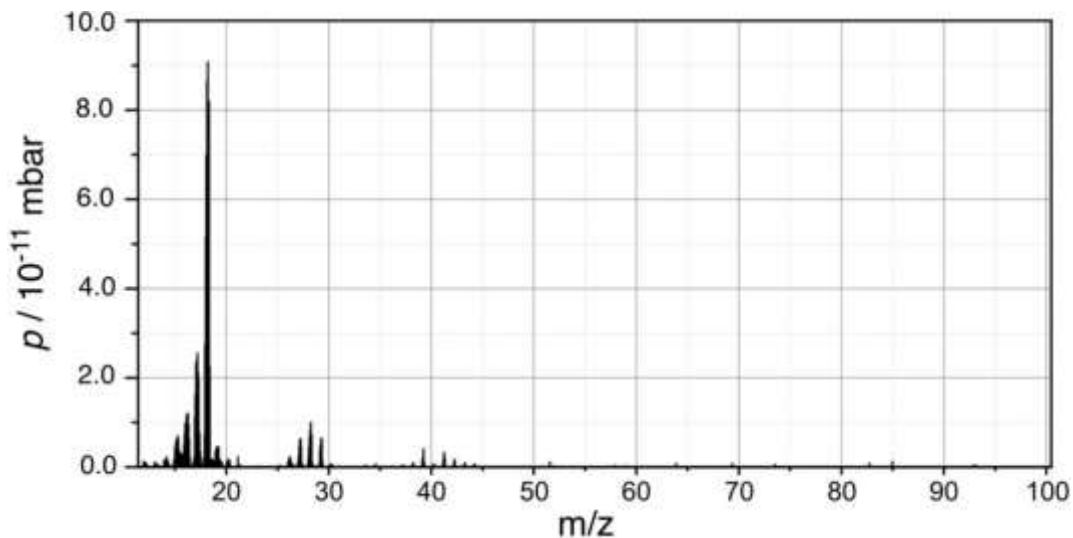


Figure S4: Mass spectrum taken during the initial warm-up phase of sample degassing at 500 K sample temperature. The spectrum was measured with an MKS e-Vision+ quadrupole mass spectrometer.

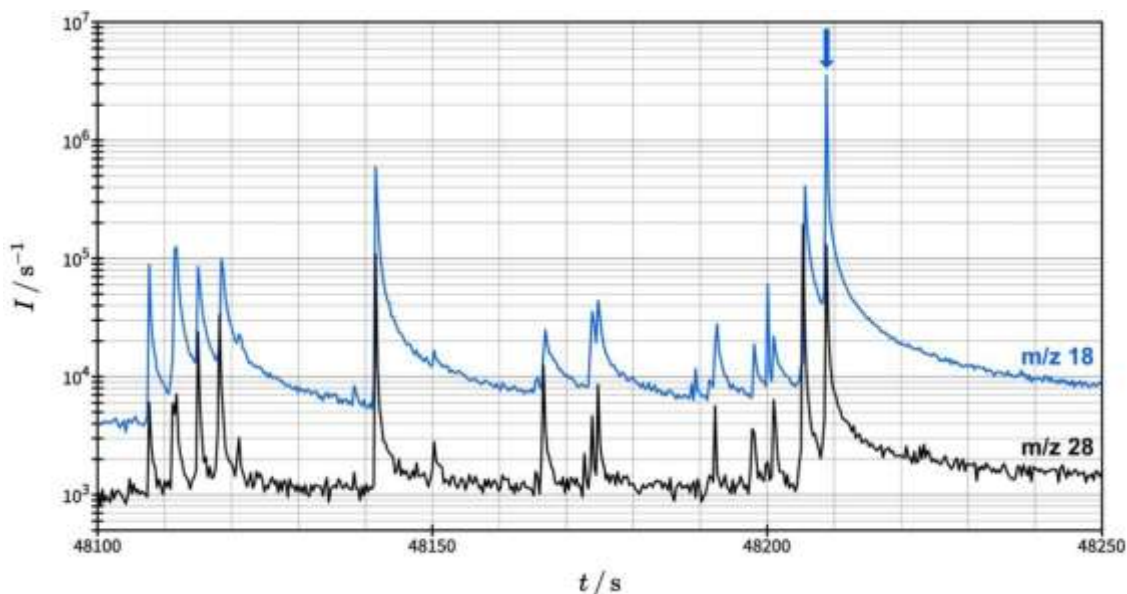


Figure S5: MID traces at m/z 18 and 28 recorded during crystal cleavage with a Hiden HAL 511 3F mass spectrometer. The traces show several spikes, which correspond to cleaving attempts. The most intense peak (marked with a blue arrow) corresponds to the final cleavage of the crystal. In total, around 35 passes with the tungsten carbide blade were needed to cleave the microcline sample.

CALIBRATION OF DESORPTION CURVES

Desorption curves shown in the main text are background corrected and calibrated. For background correction, we subtracted the weighted signal measured in the chamber from the signal measured directly above the sample surface. The intensity of the desorption rate was calibrated by referencing the known desorption curves of water desorbing from calcite (10.4). Prior to the reported experiments, we measured multiple desorption curves of water desorbing from a calcite (10.4) samples prepared as described in Ref. 18 in the main text. From these curves, we determined the desorption curves corresponding to an initial coverage of around 1.0 ML based on the appearance of the multilayer desorption peak. Then, the intensity calibration factor was calculated from the integral over the monolayer desorption curve and the known water density for a monolayer of water on calcite (see Table S1). To determine a reliable calibration factor, we averaged over the values determined from nine monolayer desorption curves measured on three different samples. The relative error of the calibration as determined from two times the standard deviation (95% confidence interval) is $\pm 11\%$. Finally, we divided the calibration factor by the water density expected for one water molecule per primitive unit cell on microcline (001) to obtain desorption rates and coverages referenced on the number of water molecules per primitive cell as shown in Figure 2.

Table S1: Characteristics of the primitive unit cell (p.c.) and adsorbed water layer on calcite (10.4) and microcline (001) used for calibration.

	Calcite (10.4)	Microcline (001)
p. c. area / m²	$4.04 \cdot 10^{-19}$	$5.56 \cdot 10^{-19}$
reference coverage	1.0 ML	0.25 ML
water / p. c.	2	1
density / m⁻²	$4.95 \cdot 10^{18}$	$1.80 \cdot 10^{18}$

ADDITIONAL TPD DATA OF WATER DESORBING FROM MICROCLINE (001)

As discussed in the main text and shown in Figure S6, the desorption curves of water desorbing from one of our microcline samples exhibit an increase in the desorption signal above 450 K. We attribute this unexpected signal increase to outgassing of water trapped inside our sample, *e.g.*, inside micropores or mineral inclusions. Water trapped inside our sample is also consistent with the sudden increase in water background pressure upon cleavage and the observation of water degassing during sample preparation (see also Ref. 17 in the main text). Moreover, the maximum intensity of the signal above 400 K does not correlate with the initial water dosage, further corroborating our assumption.

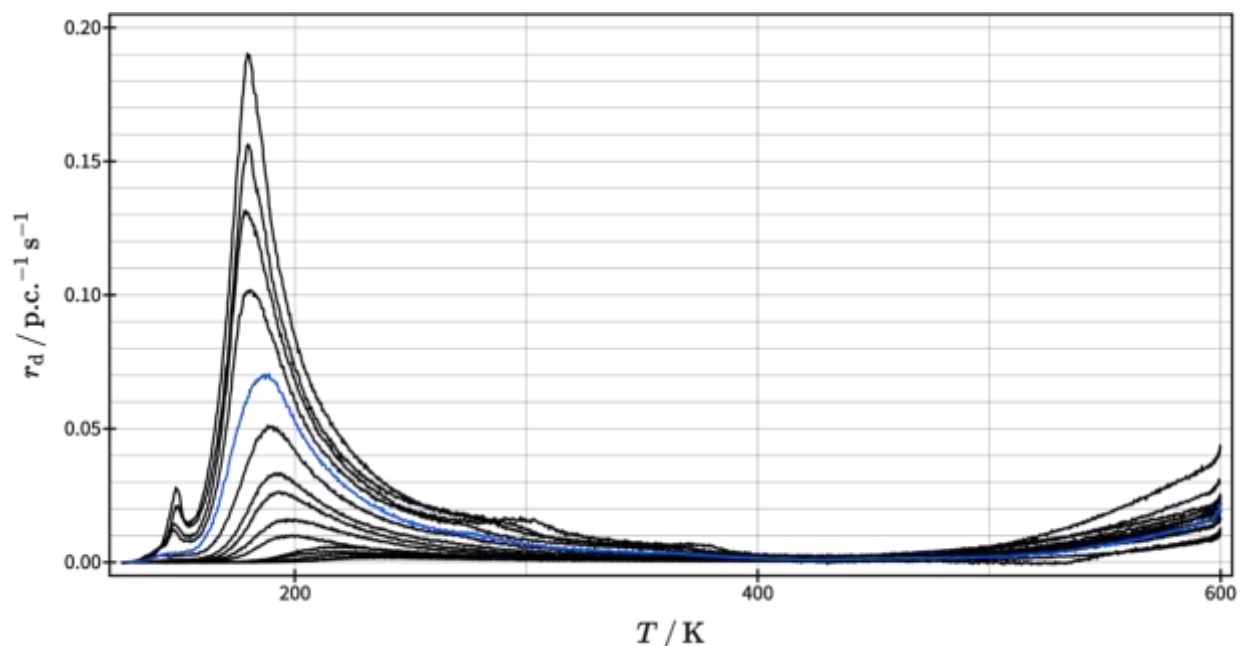


Figure S6: Full desorption curves of water desorbing from microcline (001). For the desorption curves shown in the main text, the desorption curves have been cut at 400 K. Note that the intensity of the signal increases at the end of the temperature range (above 400 K) does not correspond to the peak intensities or the dosed coverages.

For another microcline sample from the same batch, we observed the same peak structure around 200 K, but no additional increase above 450 K. Instead, the signal just decreases further towards

the end of the desorption measurement. We did, however, observe an increase in the water background upon cleavage similar to the one shown in Figure S5.

CALCULATION OF DFT ADSORPTION AND DESORPTION ENERGIES

The average adsorption energy per water molecule E_{ad} was calculated as the difference between the energy of the relaxed combined system E_{total} and the combined energies of the isolated surface E_{surf} and isolated water molecules divided by the number of water molecules per slab N (see Equation 1).

$$E_{\text{ad}} = \frac{E_{\text{total}} - (E_{\text{surf}} + N \cdot E_{\text{water}})}{N} \quad (1)$$

Next, these adsorption energies were converted into desorption energies for better comparison with the experimental TPD results. Assuming a non-activated adsorption process, the desorption energy is the negative energy difference between a system with N adsorbed molecules and a system with $N - 1$ adsorbed molecules and one molecule in the gas phase. For a very high number of molecules on the surface (as is typically the case in a TPD experiment), this is equivalent to the negative derivative of the coverage-dependent total adsorption energy $E_{\text{ad,t}}(\theta) = \theta \cdot E_{\text{ad}}(\theta)$ with respect to the coverage. To convert the adsorption energies obtained by DFT, this derivative was approximated with the differential quotient according to Equation 2 to account for the finite number of DFT energies available.

$$E_{\text{d}} = -\frac{dE_{\text{ad,t}}(\theta)}{d\theta} \approx -\frac{\theta_2 \cdot E_{\text{ad}}(\theta_2) - \theta_1 \cdot E_{\text{ad}}(\theta_1)}{\theta_2 - \theta_1} \quad (2)$$

Note that Equation 2 can be written equally for both the coverage and total number of molecules.